ORIGINAL PAPER

A synchrotron FTIR microspectroscopy investigation of fungal hyphae grown under optimal and stressed conditions

Adriana Szeghalmi · Susan Kaminskyj ·
Kathleen M. Gough

Abstract Synchrotron FTIR can provide high spatial resolution (<10 μm pixel size) in situ biochemical analyses of intact biotissues, an area of increasing importance in the post-genomic era, as gene functions and gene networks are coming under direct scrutiny. With this technique, we can simultaneously assess multiple aspects of cell biochemistry and cytoplasmic composition. In this paper, we report the first results of our synchrotron FTIR examination of hyphae of three important fungal model systems, each with sequenced genomes and a wealth of research: *Aspergillus*, *Neurospora*, and *Rhizopus*. We have analyzed the FTIR maps of *Aspergillus nidulans* cells containing the *hypA1* allele, a well-characterized single-gene temperature-sensitive morphogenetic mutation. The *hypA1* cells resemble wildtype at 28 °C but have growth defects at 42 °C. We have also investigated *Neurospora* and *Rhizopus* cultures grown in media with optimal or elevated pH. Significant differences between the spectra of the three fungi are likely related to differences in composition and structure. In addition, high spatial resolution synchrotron FTIR spectroscopy provides an outstanding method for monitoring subtle subcellular changes that accompany environmental stress.

A. Szeghalmi · K. M. Gough (✉)
Department of Chemistry, University of Manitoba,
360 Parker Building,
Winnipeg, Manitoba R3T 2N2, Canada
e-mail: kmgough@ms.umanitoba.ca

S. Kaminskyj
Department of Biology, University of Saskatchewan,
Saskatoon, Saskatchewan S7N 5E2, Canada

Introduction

Fungi have diverse impacts on the environment and on humans, in fields ranging from pathogenesis to recycling, as well as biotechnology. Many fungi are triggered by growth stress to produce metabolites that include industrially valuable and/or toxic compounds, e.g., penicillin and taxol. Novel ways of assessing fungal cell structure and composition are likely to provide valuable insights into fungal biology and will enhance our ability to understand and control fungal metabolism. We present here the first synchrotron Fourier transform infrared (FTIR) spectromicroscopic study of single fungal hyphae under optimal and stressed growth conditions, with sub-cellular spatial resolution.

The cells of filamentous fungi, including molds, grow only at their tips by means of localized secretion (exocytosis), to produce tubular cells of even width, called hyphae [1, 2]. Hyphal tips grow continuously through a complex, inter-related suite of biochemical processes. During hyphal growth, wall-forming compounds and enzymes that assist in nutrient acquisition are secreted at the extending tip. Hyphal branching, typically from subapical regions, leads to colony formation. Fungal cytoplasm is enclosed within a phospholipid cell membrane that is protected by a carbohydrate-rich wall. Newly deposited hyphal tip walls are supported from within the cell by the actin cytoskeleton; these walls differ considerably from the fully cross-linked walls in mature basal regions [3]. The apical cytoplasm contains abundant organelles, including several to many nuclei and mitochondria, thus protein-, nucleic acid-, and

lipid-rich signatures are characteristic of metabolically active regions. The apical cytoplasm actively migrates to keep up with the extending tip [4], whereas vacuoles containing various storage products predominate in basal regions. The molecular complexity and spatial variation of fungal hyphae necessitate a multifaceted strategy for their characterization.

Analytical methods have inherent tradeoffs between spatial resolution versus the number and type of components that may be analyzed. High spatial resolution histochemistry can reveal the location of target components in subcellular compartments, whereas high biochemical resolution analyses require bulk samples. FTIR spectroscopy bridges this gap, providing non-invasive biochemical characterization with spatial resolution at the sub-cellular level. Applications include FTIR spectra of fungal and plant extracts [5–9] and discrimination between fungi of different types [10–15].

Spatial resolution depends on wavelength and optical hardware; signal detection depends on sample thickness, beam intensity, and detector characteristics. Detection can be optimized by using synchrotron FTIR, providing high sensitivity with a pixel size of approximately 6 μm, which permits sub-cellular resolution of fungal hypha. Bright synchrotron sources permit acquisition of diffraction-limited spectra, where the diffraction limit is approximately inverse of the exciting wavenumber; for a typical 10×10 μm aperture, this limit is about 1,000 cm^{-1}. As the aperture is reduced further, noise increases at the longer wavelengths. Because the most important sugar bands appear in the 1,100–900 cm^{-1} region, spectra were recorded with apertures ranging from 6 to 12 μm; larger apertures were used to ensure better signal to noise, despite the associated slight decrease in spatial resolution.

Filamentous fungi are increasingly being used as experimental model systems [16–19] owing to their relatively small genomes and short life cycles, coupled with their fundamental metabolic similarity to animal systems. Genomic profiling reveals coordinate expression of suites of genes in response to changes in their environment, but does not directly address downstream events. Thus, more complete descriptions of hyphal composition have the potential to relate gene function to cellular phenotype. We show in this report that the complementary approach of high spatial resolution synchrotron FTIR permits characterization of subcellular biochemistry through in situ mapping of fungal hyphae, comparing wildtype morphologies of two Ascomycetes (Aspergillus and Neurospora) and a Zygomycete (Rhizopus). For Aspergillus, we also examined the biochemical consequences of growing an A. nidulans strain with the temperature-sensitive morphological defect, hypA1 [20–22], at permissive (28 °C) and restrictive (40 °C) temperatures. For Neurospora and Rhizopus we examined the effect of stress via growth in medium with optimal (6.5) or elevated (8.5) pH.

Materials and methods

Fungi

Experimental samples were grown from 5 mm×5 mm pieces of agar growth medium inoculated with freshly harvested spores, placed on the imaging substrate, and incubated in moist chambers for 8 to 24 h. Aspergillus nidulans strain ASK30 [20] (available from http://www.fgsc.net) was grown on supplemented complete medium buffered to pH 6.5 [23] at 28 °C or at 40 °C. Wildtype strains of Neurospora and Rhizopus, isolated from nature, were grown on pH 6.5 or pH 8.5 YG medium [23] at 28 °C. During the incubation, hyphae grew out from the agar across the imaging substrate. MirrIR low-e microscope slides (Kevley Technologies, Chesterfield, OH) or gold-coated silicon wafers (in-house, U. Manitoba) were used as substrates for FTIR. Once hyphae had grown sufficiently, samples were frozen on a metal slab at −80 °C for 30 min and dried overnight at 37 °C. A. nidulans samples were prepared and imaged with fluorescence and transmission electron microscopy as described elsewhere [21].

Synchrotron FTIR

All spectra were recorded in reflectance mode on a Nicolet 860 FTIR with Continuum microscope (NSLS), a Nicolet Magna 500 equipped with Nic-Plan microscope (SRC) or a Bruker Optics IFS66vs FTIR with Hyperion confocal microscope/mapping stage (CLS) using synchrotron radiation. Either the Nicolet OMNIC/Atlμs software or the Bruker Opus software was used for data acquisition and analyses. Typically, 64 to 128 interferograms were collected for each pixel, co-added, and ratioed to a similar background scan recorded at a blank region of the slide. Individual spectra and maps (usually line maps) were saved in $\log(1/R)$ format, 4 cm^{-1} resolution, encompassing the mid-IR region from 4,000 to 800 cm^{-1}, with zero-filling level 1. No further processing of data (e.g., smoothing or Fourier self deconvolution) was employed, to avoid the introduction of artifacts.

Individual spectra were analyzed for spectral markers of known components [5–15, 24, 25] as well as novel characteristics. Spectral data herein is displayed for single pixels; specific characteristics can also be mapped over a region or subjected to cluster analysis [25]. A CCD image of the region sampled, including a superposition of the map outline, was recorded with every map. At least 10, and as many as 30, hyphae have been investigated for each species

and growing condition, with tens to hundreds of points per sampled hypha, depending on the length of the single filament. Age and hence growth phase are determined by the distance from the tip, for each species in accordance with the specific growing conditions.

Results

Comparison of *Aspergillus nidulans*, *Rhizopus*, and *Neurospora* hyphae grown in optimal conditions

The asexual life cycle of filamentous fungi begins with spore germination and production of a vegetative hypha. Figure 1a shows the permissive phenotype of an *A. nidulans hypA1* strain following overnight growth at 28 °C, and is morphometrically similar to wildtype [20]. This specimen was stained with Hoechst 33258 to visualize DNA, and imaged with fluorescence light microscopy. The spore (S) has produced three hyphae (arrowheads). The DNA-rich nuclei appear as bright ovals, spaced at roughly even intervals. In *A. nidulans*, the position of the first nucleus and the spacing between nuclei is correlated with hyphal growth rate; the germling in Fig. 1a was growing relatively slowly.

Transmission electron microscopy of a wildtype phenotype *A. nidulans* cell, grown at 28 °C for ca. 12 h (Fig. 1b), reveals more subcellular details. The spore and hypha are surrounded by a wall that other analysis methods [1–4, 26] have shown to contain chitin, glucans, and other sugars. The cytoplasm contains a suite of organelles including many nuclei and mitochondria, as well as granules that likely contain storage products. Wildtype *A. nidulans* hyphal walls are ca. 40-nm thick [21]. The cell shown in Fig. 1b has not produced its first cross wall, which will be deposited at the spore–hypha junction. In contrast to the wildtype *A. nidulans* phenotype, Fig. 1c shows the *A. nidulans hypA1* strain, grown at 42 °C for ca. 2 d, revealing aspects of its temperature-sensitive phenotype [20] leading to distinctive non-lethal morphological abnormalities at 40–42 °C [20, 21]. The *hypA1* defect is a single base pair change in a single gene that leads to a non-conservative amino acid substitution in the HYPA gene product, hence causing HYPA instability at elevated growth temperature. The *hypA1* restrictive phenotype includes wide, slow-growing hyphae with extremely thick cell walls and aberrant cross walls [20–22]. Like wildtype, restrictive phenotype *hypA1* cells have multiple nuclei and mitochondria, as well as abundant osmiophilic granules (also seen in the germling spore in Fig. 1b) that are not typical of wildtype hyphae [21].

Aspergillus nidulans and *Neurospora* are relatively closely related (both Ascomycetes), but *Neurospora* has
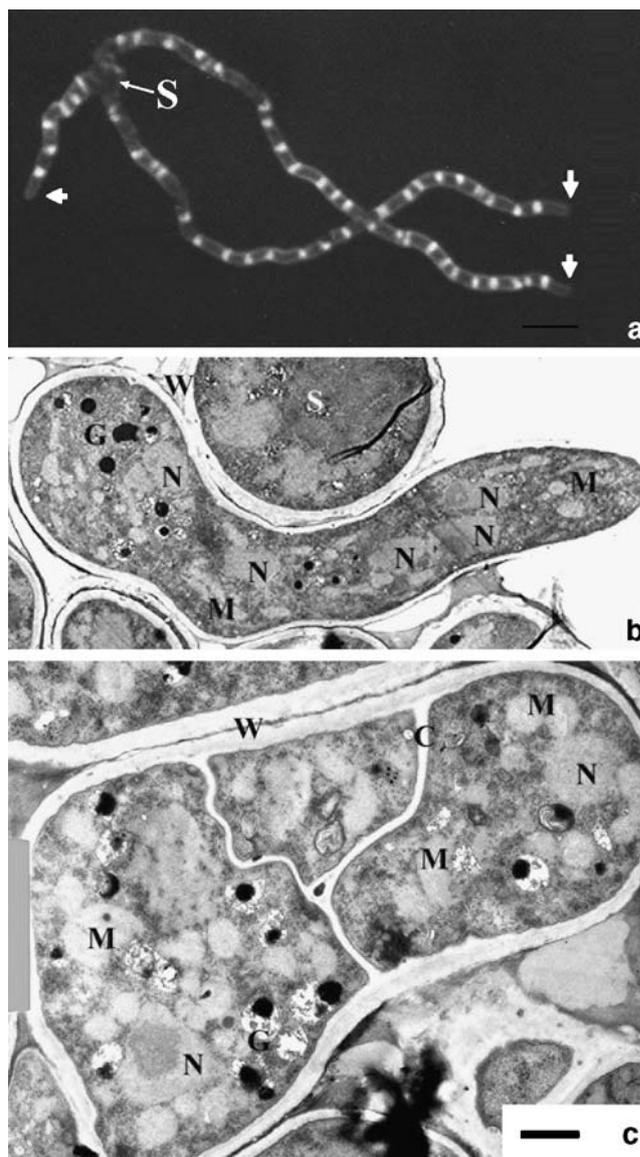

Fig. 1 Fluorescence light micrograph (**a**) and transmission electron micrographs (**b**, **c**) of *Aspergillus nidulans* strain ASK30 that contains the temperature-sensitive *hypA1* morphogenesis defect, grown at 28 °C (**a**, **b**) and (**c**) 42 °C. **a** A germling grown overnight at 28 °C, then stained with Hoechst 33258 to reveal nuclei. The spore (S) has produced three morphologically wildtype hyphae that grow only at their tips (*arrowheads*). *Bar*=5 μm. **b** A young germling whose spore (S) has germinated to produce a thin-walled (*W*) cylindrical hypha containing multiple nuclei (*N*) and mitochondria (*M*). Early growth depends on metabolites which can be stored in granules (*G*). The cell has yet to produce its first crosswall. **c** Older ASK30 cell grown at 42 °C, is much wider and has thick walls (*W*) and abnormal cross-walls (*C*). Nuclei (*N*) are similar in morphology at both growth temperatures, but mitochondria (*M*) are larger and less electron dense in cells grown at 42 °C. Unlike wildtype cells of the same age, cells of this strain grown at 42 °C also have prominent electron dense granules (*Bar*=1 μm), for B and C

three-fold wider hyphae and grows at least ten-fold faster. Although it is counter-intuitive, the broad trend for wild-type filamentous fungi is that species with wider hyphae

also tend to grow faster, but have comparably thick walls. *Rhizopus* has a similar hyphal width and growth rate to *Neurospora*, but is from a distantly related fungal group (Zygomycetes).

Figure 2 shows FTIR spectra from each of these fungi grown in optimal conditions. The spectra were acquired just behind hyphal tips, where the cell wall is newly deposited (panel A) and approximately 150 μm behind the tips, where the wall is mature. All three spectra in panel A show typical CH_2 bands at about 2,853 and 2,918 cm^{-1}, a result of the lipid bilayers in the cell and organelle membranes (mitochondria, nuclei, etc.) that support tip extension. Fungi typically contain abundant cytoplasm in the apical 100–200 μm of the hypha, behind which they become increasingly vacuolated. Vacuoles are surrounded by a single membrane and contain storage products and other metabolites.

Infrared spectroscopy has been extensively applied to differentiate between polysaccharides, in addition to protein secondary structure and lipid content, etc. [5–11, 24, 25]. FTIR spectra of model compounds show significant differences that have been interpreted on the basis of structure and bonding arrangement. Band positions for the most prominent maxima are listed in Table 1. These are reported simply as the observed maxima, rather than maxima obtained from second derivatization or from curvefits. Spectra at the tips are very low intensity, due to the small amount of material being sampled, hence the noise level is unacceptably high for the latter processes to be useful. In addition, many bands are overlapped in the region characteristic of sugars (1,150–900 cm^{-1}) and the CH stretch modes lie on a strongly sloping background from the large OH and NH stretch modes above 3,000 cm^{-1}. The amide I and II bands in the *Rhizopus* are affected by a sloping baseline that artificially lowers the position of their band maxima. Nevertheless, the maxima are sufficiently well defined for us to draw some conclusions about the biochemistry; see Discussion.

Fig. 2 FTIR spectra of *Aspergillus nidulans*, *Neurospora*, and *Rhizopus* recorded from hyphal tip (**a**) and from basal region approximately 150 μm behind tips (**b**)
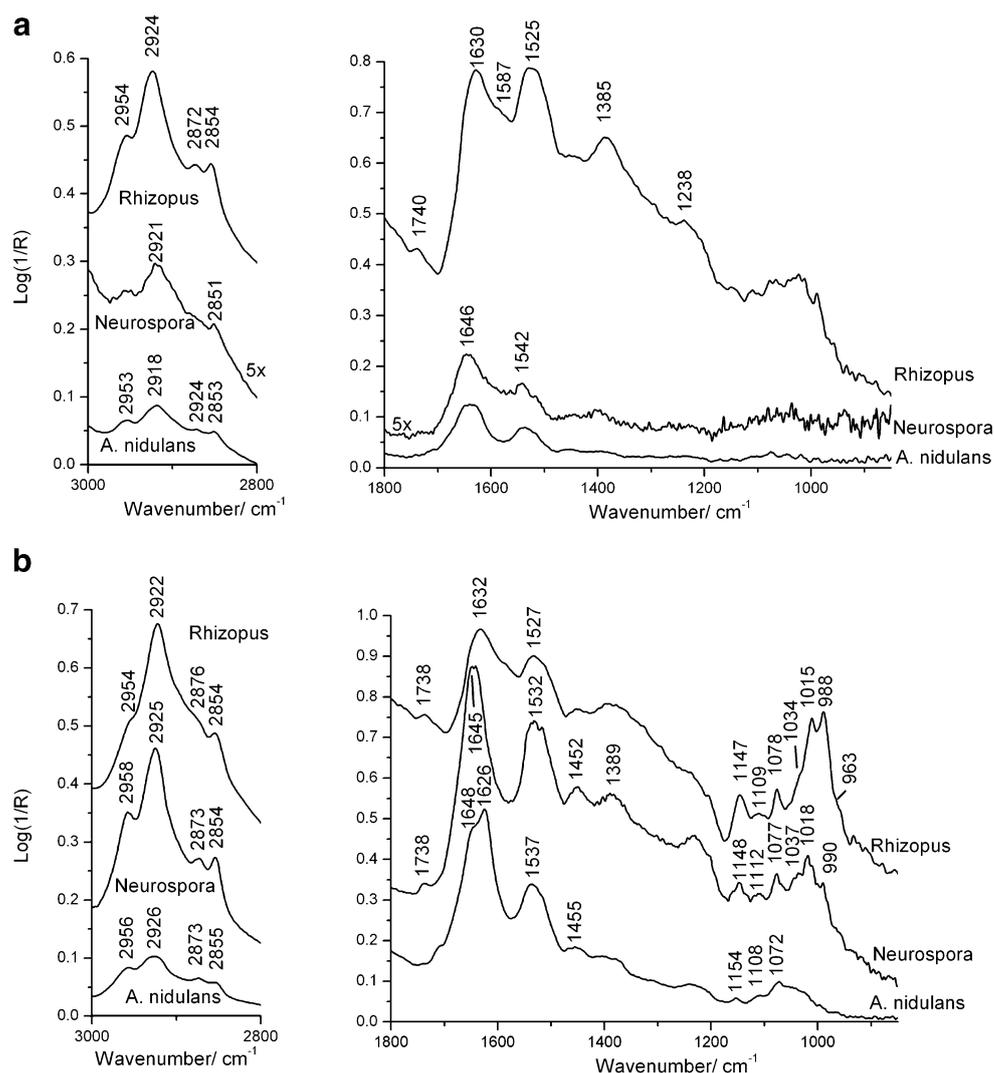
Table 1 Tentative assignment of principal FTIR absorption bands

Wavenumber (cm^{-1})	Assignment*
2,953–2,958	υ_{asym} CH$_3$ from lipids
2,918–2,924	υ_{asym} CH$_2$ from lipids
2,872–2,876	υ_{sym} CH$_3$ from lipids
2,852–2,854	υ_{sym} CH$_2$ from lipids
1,717–1,740	υ C=O
1,630–1,645	Amide I
1,587sh	Chitosan δ NH$_2$
1,525–1,539	Amide II
1,147–1,148	$\beta(1{\rightarrow}3)$ polysaccharides
1,109–1,112	$\beta(1{\rightarrow}3)$ polysaccharides
1,077–1,078	$\beta(1{\rightarrow}3)$ polysaccharides
1,034–1,037	$\beta(1{\rightarrow}3)$ glucan
1,015–1,018	Galactomannans, $\beta(1{\rightarrow}4)$ polysaccharides
988–990	$\beta(1{\rightarrow}6)$ glucans
963	Mannans

*υ stretching, δ deformation. Assignment based on refs. [5–9]

The sloping baseline is possibly due to Mie scattering [27], owing to the diameter of the hyphae being on the order of the wavelength of light employed. Such an effect has been recently suggested to occur in the case of IR spectra of nuclei in cultured human cells [28], where a similar atypical baseline was modeled by a pure scattering function. In future work, we will be exploring the use of transparent substrates so that the experiments might be performed in transmission, rather than reflection. However, the standard salt crystals used for transmission may inhibit proper fungal growth, a condition we will monitor with SEM of the hyphae.

Environmental stress: A. nidulans hypA1 grown at permissive and restrictive temperatures

Figure 3 shows FTIR spectra of the hyphal tip and of the basal region of the permissive (A) and restrictive (B) *A. nidulans hypA1* phenotypes. Panel A shows wildtype phenotype spectra that illustrate changes that occur during hyphal maturation. Panel B shows spectra for the restrictive phenotype of the *A. nidulans hypA1* strain. Since the rate of *hypA1* cell growth is greatly slowed at the elevated temperature, a much shorter hypha is produced, necessitating fewer points to represent a similar time scale (panel B).

Environmental stress: Rhizopus and Neurospora grown at optimal and elevated pH

Fungal growth medium typically has slightly acidic pH; consequently, growth in slightly alkaline medium causes metabolic stress. During growth, fungi secrete organic acids in part to acquire certain nutrients, and incidentally modifying their environmental pH. The range of growth medium pH is relatively broad, but in general growth rate on somewhat alkaline medium is slower and the cells are less robust. Many of the biochemical consequences of pH stress are poorly understood.

In our experiments, both *Neurospora* and *Rhizopus* were severely affected by the change from optimal to elevated growth medium pH. At elevated pH, hyphal growth was slow and sparse, although morphologically wildtype. Many of the hyphal tips were vacuolate or ruptured during preparation, unlike growth at optimal pH. Representative data are shown in Fig. 4 (*Neurospora*) and Fig. 5 (*Rhizopus*). In Fig. 4, panel A, we show the photomicrograph and FTIR spectra from tip to 200 μm for *Neurospora* grown at pH 6.5. Band positions are labeled primarily for the 200 μm analysis point, where the sugar region of the spectrum is more intense and several bands are well defined. Panel B of Fig. 4 depicts a *Neurospora* hypha grown at pH 8.5. The photomicrograph shows these hyphae have similar appearance; however, the spectra are quite different. Most notably the pH-stressed *Neurospora* lacked any strong signals in the sugar region, consistent with the reduced growth vigor and increased wall fragility.

Figure 5 presents similar data for the *Rhizopus*, with panel A showing the photomicrograph and FTIR spectra of a hypha grown at pH 6.5, and panel B showing comparable data for a hypha grown at pH 8.5. The results here are more dramatic, in that the *Rhizopus* hyphae grown at pH 6.5 exhibit a strong sugar signal almost immediately from the tip, whereas the pH-stressed hypha fails to establish this spectral signature. The morphological structure mirrors this behavior (vide infra). Furthermore, this hypha shows a dramatic loss of protein signal between 30 and 50 μm behind the tip, consistent with the collapsed basal part of this cell.

Figure 6 shows another example of a pH-stressed *Rhizopus* hypha that contains exceptionally interesting information on fungal behavior. At different times, several hyphal tips grew from the agar block, which is out of view on the left-hand side of the image. The first of these hyphae grew across the field of view to the lower right-hand corner. Spectra 1 and 2 were taken from the collapsed region of this first cell. Later, a second hypha grew along the collapsed remains of the first, extending to where spectrum 3 was acquired. This hyphal tip also seems to have aborted, since it appears to be collapsed, and the spectra from 3–7, while considerably stronger in the amide I and II bands than spectra 1 and 2, are still very weak. Finally, additional hyphae grew along the track of the first two (Fig. 6, point 8). The features in spectrum 8 are intermediate between those of the optimal growth hypha at tip and 20 μm shown in Fig. 5a.

Fig. 3 Photomicrographs and FTIR spectra acquired along hyphae of permissive (**a**) and restrictive (**b**) *A. nidulans hypA1* phenotypes. *Scale bars* 50 μm
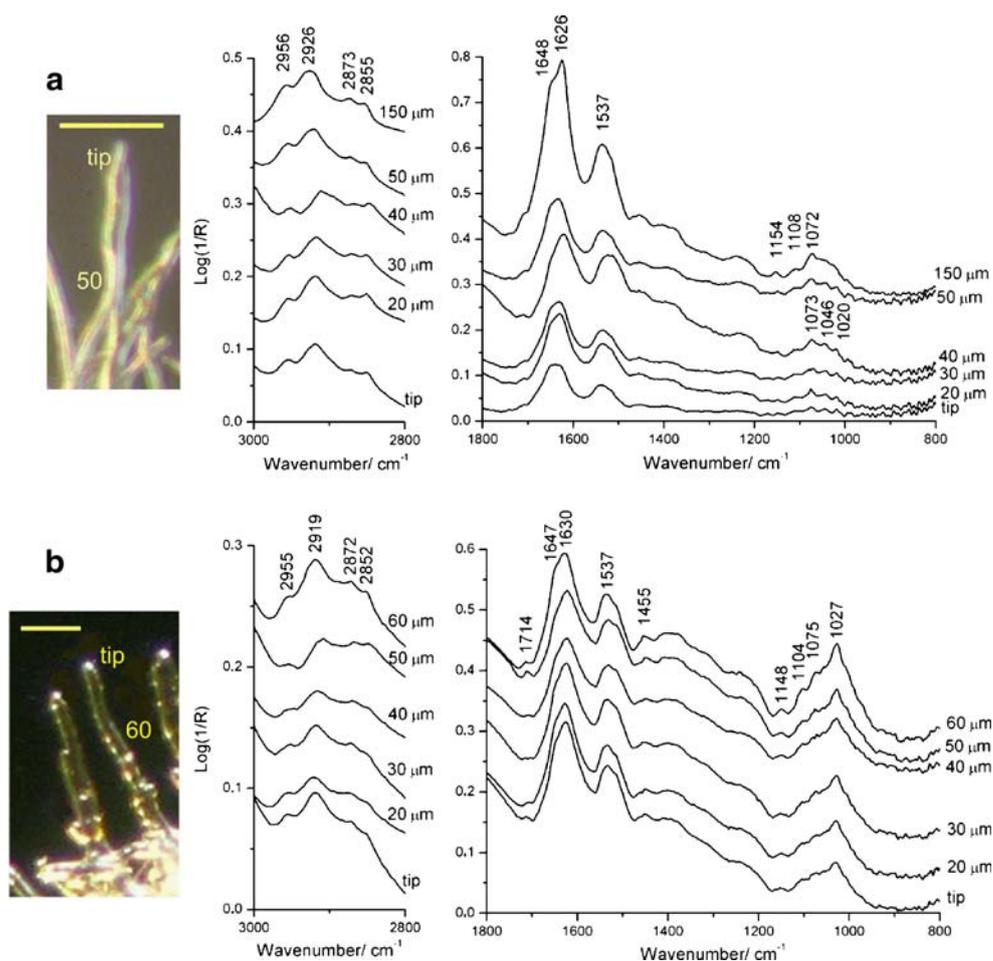

Discussion

Fungi have wide ranging impacts on the environment and on humans, and as they have tractable genomes and growth characteristics, they are both amenable and important to study. Fungi are an emerging threat for human health, especially for immune-compromised and HIV patients, particularly as humans and fungi have overall similar metabolism [16–18]. Anti-fungal drugs are toxic, expensive, cure rates are low, and cures seldom last more than a few months. Fungal plant pathogens are the most important threat to the global food supply [19]. Fungal–plant root interactions called mycorrhizae are thought to have been essential for emergence of plants onto land ca. 450 million years ago, and currently mycorrhizae are associated with 95% of plant species [29]. The high level of genetic conservation between fungal species [16–18] means that knowledge from one system is often readily transferable. However, we show here that genetic conservation amongst fungi does not preclude substantial differences in cell composition, nor in variations in response to environmental stress (e.g., growth of *Neurospora* and *Rhizopus* at elevated pH).

Variation in cell composition is fundamentally related to the organism's ability to carry out specialized functions in appropriate regions. Many organelles have chemically distinctive components (nucleic acids, proteins, carbohydrates, and lipids) in characteristic proportions, so a high spatial resolution spectral/biochemical map of a cell can also provide ultrastructural information. While more precise chemical identification is possible with liquid or gas chromatography and mass spectrometry, such techniques require homogenized samples, thus all spatial resolution is lost. High spatial resolution in situ chemical analyses using synchrotron FTIR can simultaneously assess multiple aspects of cell biochemistry and cytoplasmic structure. Here, we have used high spatial resolution synchrotron FTIR to examine hyphal composition in three fungal genera: *Aspergillus*, *Neurospora*, and *Rhizopus*. All are important fungal model systems with sequenced genomes and a wealth of research.

Strong differences in cell composition are immediately obvious in the FTIR spectra of *Neurospora* and *Rhizopus* and the wildtype morphology *A. nidulans hypA1* cells grown under permissive conditions. Wildtype *A. nidulans* hyphae are narrow, typically 3-μm wide, whereas *Neurospora* and *Rhizopus* hyphae are about 10-μm wide. Thus, the

Fig. 4 Photomicrographs and FTIR spectra acquired along *Neurospora* hyphae grown at pH 6.5 (**a**) and pH 8.5 (**b**). *Scale bars* 50 μm
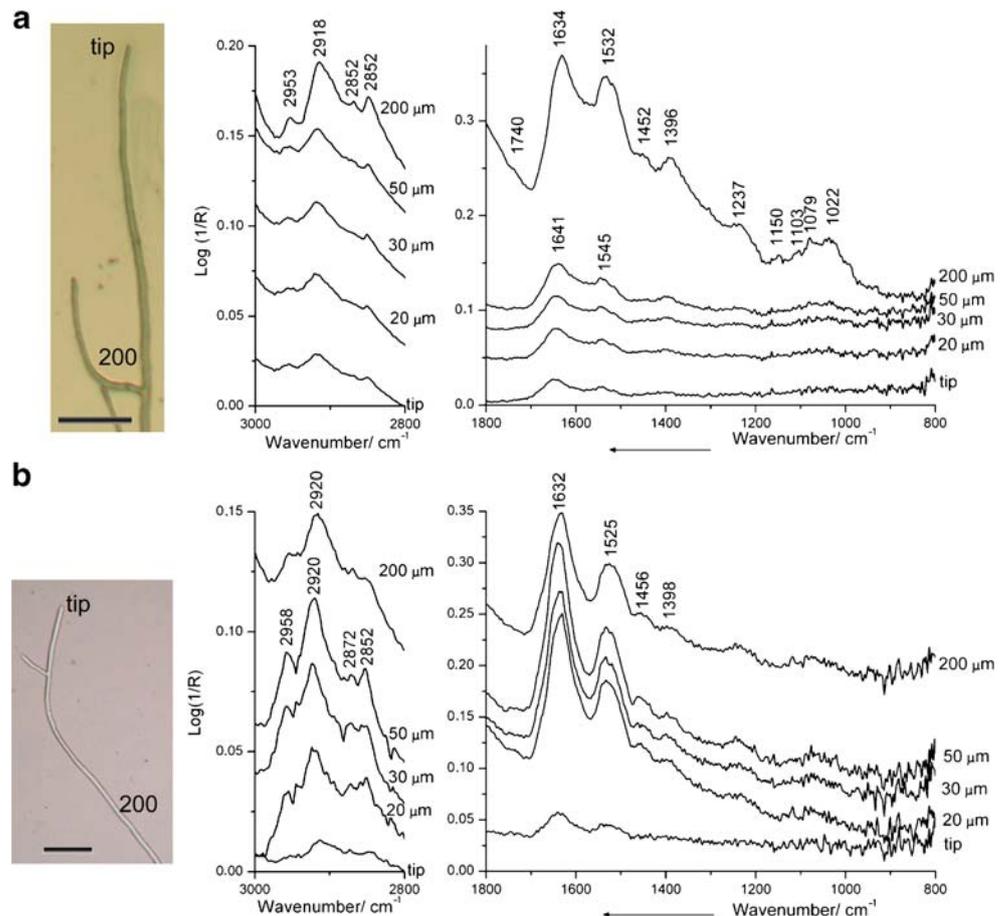
volume per unit length for a wildtype *A. nidulans* hypha is about 10% that of *Neurospora* or *Rhizopus* hyphae, which will substantially change the strength of the spectra. The *A. nidulans* wildtype spectra have lower total signal, primarily protein (strong amide I and II bands around 1,645 and 1,536 cm^{-1}). These band positions are slightly lower than those reported for hyphal extracts [9–14] and may be indicative of multiple and disordered protein conformations in the growing hyphae, for example due to transitions between active and inactive protein conformation states in the evolving, growing hyphae. However, as the baselines were often not very flat, possibly due to scattering (see above), these positions may not be very accurate. In addition, signals from *N*-acetylated glucosamines in the cell wall matrix will confound the interpretation in this region. Fungal hyphal tips contain the proteins and organelles required to fuel growth, plus wall matrix materials that together with the fibrils synthesized in situ will create the mature wall. Using FTIR, it is not possible to distinguish between cytoplasm and wall components. The sugar spectra at hyphal tips are the sum of the forming and mature wall that ensheath the cell membrane, wall matrix components being synthesized in the apical cytoplasm that have yet to be secreted at the tip, and short-term metabolic stores in the apical cytoplasm.

The larger size of *Neurospora* and *Rhizopus* hyphae and, quite likely, species-specific biochemical differences result in a much stronger series of absorptions in the sugar region (1,100–900 cm^{-1}). *Rhizopus* has the highest sugar content among the investigated fungi, consistent with the use of this fungus as an alternative for natural chitin and chitosan production as its cell wall is rich in these biopolymers [30]. Differences in band position and intensity are indicative of differences in cell wall composition. Thus, as has been noted by others [10–14], FTIR spectroscopy could become a feasible technique to differentiate these particular fungi and hence could have quality control applications.

We compared growth of the *A. nidulans* *hypA1* temperature-sensitive morphogenesis allele grown at permissive (28 °C) and restrictive (40 °C) temperatures. Comparisons between wildtype and mutant strains of a given species do not follow general trends. *A. nidulans* *hypA1* cells grown at 40–42 °C have at least four-fold thicker walls [21] and three-fold wider cells [20] than those grown at 28 °C, but their growth rate at 40–42 °C is approximately 1% that at 28 °C [20].

The apical cytoplasm of 28 °C-grown *A. nidulans* hyphae is protein- and nucleic acid-rich in terms of the organelles present, but the hyphae are narrow and so have relatively low biomass. There are clear differences between

Fig. 5 Photomicrographs and FTIR spectra acquired along *Rhizopus* hyphae grown at pH 6.5 (**a**) and pH 8.5 (**b**). *Scale bars* 50 μm
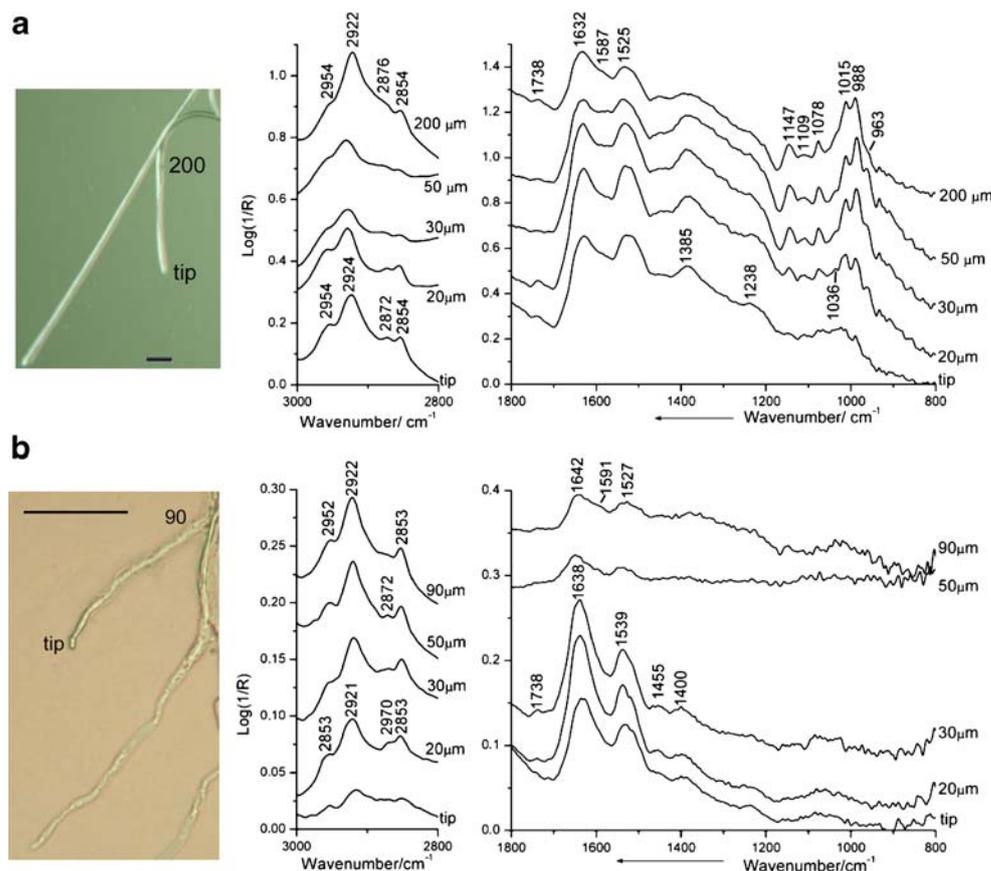

the cytoplasmic components in tip and basal regions in the cell. FTIR spectra clearly correspond to this spatial layout (Fig. 3a). Major differences are seen in the sugars, likely due in part to the presence of chitin microfibrils that are synthesized in situ from membrane-localized enzyme synthetic complexes deposited as the hypha extends. Differences are also seen in the protein and lipid peaks, probably due to changes in the organelle complement. The first nucleus in this cell is likely situated circa 12 μm behind the tip, based on the intensity of the phosphate stretch band. There is almost no signal from the tip, and it is mainly protein likely in part due to the internal, supporting actin cytoskeletal arrays. There is an increase in the protein, phosphate, sugar, and lipid content 12 μm behind the tip, consistent with the hypha having reached its full width and organelle complement. The intensity of the protein, phosphate, and lipid bands falls with distance from the tip, consistent with basal regions of hyphae being increasingly vacuolate. Hence, consistent with previous studies [1, 2] the distance from the tip correlates well with hyphal age. The cytoplasm exhibits apex-directed migration within the tube wall, following the growing tip [4].

A. nidulans hypA1 cells grown at elevated temperature have a high content of carbohydrates, proteins, and nucleic acids, even at the tip (FTIR spectra Fig. 3b). *A. nidulans hypA1* cells grown at 40 °C have comparable thickness to

Neurospora hyphae, plus blunter tips with thicker walls, and both are Ascomycetes, consistent with similar signal intensity. We also found that the *A. nidulans hypA1* cells grown at 40 °C had similar composition and quantity (signal intensity) of cytoplasm down the length of the hyphae. In addition, the FTIR band intensities for the restrictive phenotype are considerably higher, as expected, since these cells are about three-fold wider than the permissive phenotype and have a substantially thicker cell wall. Restrictive phenotype cells have many nuclei (see ref. [20]), which also is apparent in the strong phosphate band. Unlike the permissive phenotype, the *A. nidulans hypA1* restrictive phenotype includes increasing cell width with distance behind the hyphal tip, so these aberrant growing regions typically contain organelle-rich cytoplasm throughout, and lack vacuolate basal regions.

A major strength of molecular DNA manipulation of organisms is its precision. Thereafter, precise manipulations must be interpreted in the context of organismal response. Often, gene deletions are said to have no phenotype, which means we cannot detect a difference under the growth conditions used. Using FTIR we can examine the effect of a precise genetic change on cellular metabolism. Our *Aspergillus nidulans* A28 and ASK30 strains differ by a single DNA basepair change in a non-essential gene, leading to morphological consequences at elevated growth tem-

Fig. 6 Photomicrograph and FTIR spectra of *Rhizopus* grown at pH 8.5. Spectra *1* and *2* were recorded on the track of a collapsed hyphae. Spectra *3–7* were acquired from a new tip growing along the collapsed one, and spectrum *8* from the basal region of overlapping hyphae. *Scale bar* 50 μm
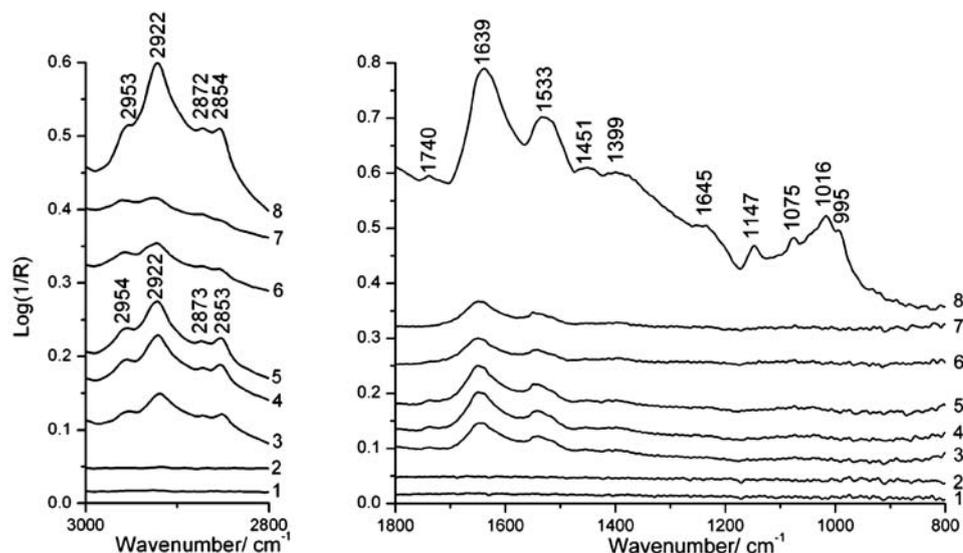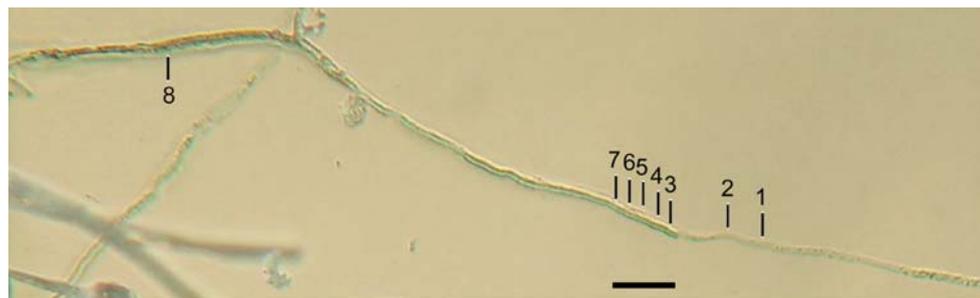
perature. Under normal (permissive) growth conditions we cannot detect a difference between these strains, i.e., there is 'no permissive phenotype'. More generally, these results show that synchrotron FTIR will be a valuable addition to a suite of analyses, including genome array profiling and structural studies.

Synchrotron FTIR results will help guide experiments to resolve contradictory data reported from other techniques: electron microscopy shows abundant electron dense, possibly osmiophilic, granules within membranous whorls in the *A. nidulans hypA1* cells grown at 42 °C, compared to the 28 °C cells. The granules have been interpreted as membrane aggregates [20], since membranes are osmiophilic. However, confocal microscopy of similarly grown cells probed with membrane-selective fluorescent markers does not detect abundant endomembranes ([22] and Kaminskyj unpublished results). Our FTIR results show that *hypA1* cells grown at 40 °C do not have unusually high lipid content compared to those grown at 28 °C, indeed almost the opposite. Thus we have reason to be more confident in the confocal microscopy results and conclude that there must be another reason for the granule electron density. Candidate compounds include protein and polyphosphate, both of which have FTIR spectroscopic support. Polyphos-

phate accumulations can be detected with histochemical methods, and/or with electron-energy loss transmission electron microscopy, which will be used to resolve this issue.

We have also compared growth of *Rhizopus* and *Neurospora* on media with pH 6.5 or 8.5. The latter caused stress, impaired cell wall construction, and reduced growth rate. Here again, the FTIR spectra permit us to make new observations about their growth, composition, and response to pH stress.

Neurospora

Fungal cells respond to environmental stress by changing their morphology and/or biochemistry. For example, although its growth optimum is in pH 6.5 medium, *Neurospora* can grow in media with a relatively broad pH range, but at the extremes its growth is slow and morphologically abnormal. Growth in less extreme conditions is still likely to have an effect, but can be more difficult to monitor. This is biologically relevant, since many industrial strains are grown under particular conditions in order to generate a desired product.

Apical regions of *Neurospora* hyphae grown at pH 6.5 have stronger FTIR spectra than *A. nidulans*, presumably

due to increased width. Thus, *Neurospora* nuclei and mito-chondria are more abundant than in *A. nidulans* and have a different arrangement consistent with the hyphae being wider. High mitochondrial and metabolite abundance are needed to fuel the fast tip growth in the species. The FTIR spectra of unstressed hyphae (Fig. 4a) are consistent with this interpretation, as the *Neurospora* has stronger carbohydrate peaks at 100 and 200 μm behind the tip than are found in the corresponding regions of the *A. nidulans* (Fig. 3a).

Unexpectedly, when *Neurospora* was grown at pH 8.5, which caused significantly slower growth, the carbohydrate content of the walls was reduced. Although the appearance of stressed hyphae in Fig. 4b is comparable to the un-stressed hyphae in Fig. 4a, there are striking differences in the FTIR spectra. The protein signal (amide I and II) is stronger in the pH stressed hypha; $\log 1/R$ for the amide I is about 0.15 compared to 0.07 in the normal hypha, in the first 50 μm. Perhaps more importantly, there is no evidence of carbohydrate enrichment (in walls, in wall-forming vesicles prior to exocytosis, and as metabolites) in the apical 200 μm of the hypha. Likely these responses include coordinated changes in metabolic rate, cytoplasmic motility, secretion rate, and wall composition. These relatively minor pH-induced changes collectively lead to a debilitated cell with slow growth and weakened walls, despite it being able to maintain a relatively wildtype appearance.

Rhizopus

Rhizopus has a similar hyphal width and growth rate to *Neurospora*, but although they are both true fungi, these species are taxonomically distant. Compared to the two ascomycetes, *Rhizopus* hyphae had considerably higher protein content in apical regions, 5–200 μm from the tip (Figs. 2 and 5a). Note that, in *Rhizopus*, the bands in the sugar region are intense and well defined, indicative of a more robust carbohydrate chemistry that may be ascribed to a combination of carbohydrate synthesis within the cyto-plasm as well as completed wall.

However, like *Neurospora*, the carbohydrate content of the *Rhizopus* hyphae was dramatically reduced when grown at pH 8.5. In the case of the *Rhizopus*, this was also shown by increased cell wall breakage in basal regions (photomi-crograph in Fig. 5, panel B) and increased frequency of tip rupture (not shown). The FTIR spectra show the biochem-ical consequences of the pH stress (Fig. 5b), most notably an almost complete absence of signal in the sugar region ($1,100–900$ cm^{-1}) that was so richly present at an early stage in the normal hypha (Fig. 5a).

The majority of the pH-stressed *Rhizopus* hyphae failed to establish a wildtype growth pattern. Many of the hyphae extended outward for several hundred μm from the growth medium block, but then appeared to have collapsed, leaving behind a trail of dessicated, broken cell constituents. Interestingly, we discovered new hyphae in which the young tip followed the path of the older dead cell (Fig. 6). A plausible interpretation is that this is a direct response to achieve survival in the pH-stressed environment, as there would be more nutrients in the dead hypha, and possibly a more amenable pH. The FTIR spectra support this interpretation. There is little signal along the path of the failed hypha (spectra 1 and 2, and similar spectra for approximately 200 μm further out) with the exception of the occasional increase in signal where some detritus remains adhering to the slide. At point 3, there is a dramatic increase in signal; the spectrum is more similar to that of a normal, unstressed growing tip. The amide I signal has an intensity of about 0.05, much weaker than that observed in the unstressed hypha. However, in this instance, the signal in the $1,000–900$ cm^{-1} region remains weak, indicating that cell wall remained somehow abnormal. About 300 μm further back, we find evidence that a more normal cell wall has been established, perhaps the presence of another, still-growing tip. The FTIR spectrum (point 8) shows medium-intensity sugar bands indicative of cell wall formation. The composition of the cell still differs from the unstressed system. In the healthy *Rhizopus* hyphae, the strongest band appears at 988 cm^{-1}, possibly corresponding to sugars with $\beta(1{\rightarrow}6)$ glucans, whereas at pH 8.5, this band is much weaker. The shoulder at $1,585$ cm^{-1} in the normal hypha, and likely due to chitin and chitosan components, is also absent in the pH-stressed hyphae. Even so, these results demonstrate the robustness and adaptability of fungi towards overcoming environmental stress.

Conclusions

Synchrotron FTIR provides a powerful tool for probing the biochemical effect of gene function, as well as en-abling us to integrate, inform, and direct other experi-mental modes. Through comparison of wildtype hyphae at different distances from the hyphal tip, we have shown differences in cell composition, previously assessed only for specific organelles (e.g., nuclei) or components (e.g., walls). Consistent with general results from light, SEM, and TEM microscopic studies, FTIR spectra show that cytoplasm near the apical tip contains more protein- and membrane-rich organelles than older regions, where cells are vacuolated.

Comparison between wildtype and mutant phenotype *A. nidulans* hyphae, which differed only in the temperature at which they were grown, shows the multiple downstream effects from a single genetic lesion. FTIR spectra of both of the fungi maintained in elevated pH growth medium identified severe alteration in the sugar composition of

these fungi when compared with the corresponding non-pH-stressed culture. This alteration was associated with damaged cell walls which eventually disintegrate. Some hyphae yet survive, by means of over-growing the paths left by failed hyphae. They establish successful growth by feeding on the residual organellar material, and may be assisted by the presence of organic acids secreted by the failed hypha. This is the converse of what happened when *A. nidulans hypA1* was grown at restrictive temperature, showing that cellular accommodation to stress can take many different forms.

References

1. Heath IB (ed) (1990) Tip growth in plant and fungal cells. Academic Press, Toronto
2. Gow NAR, Gadd GM (eds) (1995) The growing fungus. Chapman and Hall, London
3. Heath IB, Kaminskyj S (1989) J Cell Science 93:41–52
4. Kaminskyj S, Heath IB (1996) Mycologia 88:20–37
5. Michell AJ, Scurfield G (1970) Aust J Biol Sci 23:345–360
6. Sandula J, Kogan G, Kakurakova M, Machova E (1999) Carbohydr Polym 38:247–253
7. Kacurakova M, Capek P, Sasinkova V, Wellner N, Ebringerova A (2000) Carbohydr Polym 43:195–203
8. Bahmed K, Quiles F, Bonaly R, Coulon J (2003) Biomacromolecules 4:1763–1772
9. Wang Y, Zhang M, Ruan D, Shashkov AS, Kilcoyne M, Savage AV, Zhang L (2004) Carbohydr Res 339:327–334
10. Naumann D, Helm D, Labishinski H (1991) Nature 351:81–82
11. Galichet A, Sockalingum GD, Belardi A, Manfait M (2001) FEMS Microbiol Lett 197:179–186
12. Mohacek-Grosev V, Bozac R, Pupples GJ (2001) Spectrochim Acta A 57:2815–2829
13. Essendoubi M, Toubas D, Bouzaggou M, Pinon JM, Manfait M, Sockalingum GD (2005) Biochim Biophys Acta 1724:239–247
14. Fischer G, Braun S, Thissen R, Dott W (2006) J Microbiol Methods 64:63–77
15. Adt I, Toubas D, Pinon JM, Manfait M, Sockalingum GD (2006) Arch Microbiol 185:227–285
16. Galagan JE, Calvo SE, Cuomo C, Ma LJ, Wortman JR, Batzoglou S, Lee SI, Basturkmen M, Spevak CC, Clutterbuck J, Kapitonov V, Jurka J, Scazzocchio C, Farman M, Butler J, Purcel S, Harris S, Braus GH, Draht O, Busch S, d'Enfert C, Bouchier C, Goldman GH, Bell-Pedersen D, Griffiths-Jones S, Doonan JH, Yu J, Vienken K, Pain A, Freitag M, Selker EU, Archer DB, Penalva MA, Oakley BR, Momany M, Tanaka T, Kumagai T, Asai K, Machida M, Nierman WC, Denning DW, Caddick M, Hynes M, Paoletti M, Fischer R, Miller B, Dyer P, Sach MS, Osmani SA, Birren BW (2005) Nature 438:1105–1115
17. Denning DW, Anderson MJ, Turner G, Latge JP, Bennett JW (2002) Lancet Infect Dis 2:251–253
18. Galagan JE, Calvo SE, Borkovich KA, Selker EU, Read ND, Jaffe D, FitzHugh W, Ma LJ, Smirnov S, Purcell S, Rehman B, Elkins T, Engels R, Wang S, Nielsen CB, Butler J, Endrizzi M, Qui D, Ianakiev P, Bell-Pedersen D, Nelson MA, Werner-Washburne M, Selitrennikoff CP, Kinsey JA, Braun EL, Zelter A, Schulte U, Kothe GO, Jedd G, Mewes W, Staben C, Marcotte E, Greenberg D, Roy A, Foley K, Naylor J, Stange-Thomann N, Barrett R, Gnerre S, Kamal M, Kamvysselis M, Mauceli E, Bielke C, Rudd S, Frishman D, Krystofova S, Rasmussen C, Metzenberg RL, Perkins DD, Kroken S, Cogoni C, Macino G, Catcheside D, Li W, Pratt RJ, Osmani SA, DeSouza CPC, Glass L, Orbach MJ, Berglund A, Voelker R, Yarden O, Plamann M, Seiler S, Dunlap J, Radford A, Aramayo R, Natvig DO, Alex LA, Mannhaupt G, Ebbole DJ, Freitag M, Paulsen I, Sachs MS, Lander ES, Nusbaum C, Birren B (2003) Nature 422:859–868
19. Dean RA, Talbot NJ, Ebbole DJ, Farman ML, Mitchell TK, Orbach MJ, Thon M, Kulkarni R, Xu JR, Pan H, Read ND, Lee YH, Carbone I, Brown D, Oh YY, Donofrio N, Jeong JS, Soanes DM, Djonovic S, Kolomiets E, Rehmeyer C, Li W, Harding M, Kim S, Lebrun MH, Bohnert H, Coughlan S, Butler J, Calvo S, Ma LJ, Nicol R, Purcell S, Nusbaum C, Galagan JE, Birren BW (2005) Nature 434:980–986
20. Kaminskyj S, Hamer J (1998) Genetics 148:669–680
21. Kaminskyj S, Boire M (2004) Can J Bot 82:807–814
22. Shi X, Sha Y, Kaminskyj S (2004) Fungal Genet Biol 41:75–88
23. Kaminskyj S (2001) Fungal Genetics Newsletter 48:25–31
24. Gough KM, Zelinski D, Wiens R, Rak M, Dixon IMC (2003) Anal Biochem 316:232–242
25. Gough KM, Rak M, Bookatz A, Del Bigio M, Mai S, Westaway D (2005) Vib Spectrosc 38:133–141
26. Hill TW, Loprete DM, Momany M, Ha Y, Harsch LM., Livesay JA, Mirchandani A, Murdock JJ, Vaughn MJ, Watt MB (2006) Mycologia 98:400–410
27. Mie G (1908) Ang Phys (Leipzig) 25:377–452
28. Mohlenhoff B, Romeo M, Diem M, Wood BR (2005) Biophys J 88:3635–3640
29. Smith SE, Read DJ (1997) Mycorrhizal symbiosis, 2nd edn. Academic Press, NY
30. Tan SC, Tan TK, Wong SM, Khor E (1996) Carbohydr Polym 30:239–242